



ELSEVIER

Nuclear Physics A722 (2003) 273c–278c



[www.elsevier.com/locate/npe](http://www.elsevier.com/locate/npe)

## Heavy nuclei studied in projectile fragmentation

Zs. Podolyák<sup>a</sup>, P.H. Regan<sup>a</sup>, P.M. Walker<sup>a</sup>, M. Caamãno<sup>a</sup>, K. Gladnishki<sup>a</sup>, J. Gerl<sup>b</sup>,  
M. Hellström<sup>b</sup>, P. Mayet<sup>b</sup>, M. Pfützner<sup>c</sup>, M. Mineva<sup>d</sup> for the GSI ISOMER collaboration

<sup>a</sup>Department of Physics, University of Surrey, Guildford GU2 7XH, United Kingdom

<sup>b</sup>GSI, Planckstrasse 1, D-64291 Darmstadt, Germany

<sup>c</sup>Institute of Experimental Physics, Warsaw University, Pl-00861 Warsaw, Poland

<sup>d</sup>Div. of Cosmic and Subatomic Physics, Lund University, SE-22100 Lund, Sweden

The structure of heavy nuclei has been investigated in GSI by means of  $\gamma$ -ray isomer spectroscopy following projectile fragmentation. The obtained results as well as experimental aspects relevant for further studies are discussed.

### 1. INTRODUCTION

Projectile fragmentation has proved to be an effective tool in the population of exotic nuclei on both sides of the valley of stability [1–3]. Intermediate energy (50–150 MeV  $\times$  A) projectile fragmentation facilities operate in RIKEN (Japan), GANIL (France), MSU (USA) and Lanzhou (China), allowing the study of light and medium mass nuclei. A large number of different types of experiments have been performed in these laboratories, including interaction cross section measurements [1], Coulomb excitation [4,5], isomeric decay [6],  $\gamma$ -ray spectroscopy at the production target [7,8], g-factor measurements of ground [9] and excited states [10], secondary fragmentation [11,12], two-proton decay [13] etc. However, in order to study heavy systems, higher-energy accelerators and a fragment separator with the appropriate specifications are needed [14], presently available only in GSI (Germany). High-energy projectile fragmentation was used to study halo nuclei [15], g-factors [16], Coulomb excitation of light nuclei [17], isomeric decays [18–20], two-proton decay [21] etc. We note that the same experimental setup can be used to study nuclei following projectile-fission [22,23].

In this paper we review the results obtained on heavy nuclei ( $Z > 60$ ) produced in projectile fragmentation. These experiments are currently limited to studies of isomeric decays. The method allows the study of excited states only in those nuclei which are produced during the fragmentation process in isomeric states, with in-flight lifetimes long enough ( $>100$  ns) to survive the time of transportation between the production target and the  $\gamma$ -ray detection system. The upper limit on the half-life, to obtain fragment- $\gamma$ -ray correlations, is about 1 ms, which excludes most  $\beta$ -decay studies.

## 2. EXPERIMENTAL SETUP

A high energy ( $\approx 1 \text{ GeV} \times A$ ) heavy ion beam (typically either  $^{208}\text{Pb}$  or  $^{238}\text{U}$ ) was fragmented on a thick target. The nuclei of interest were separated and identified using the FRagment Separator (FRS) [14] operated in achromatic mode with a wedge-shaped aluminium degrader placed at the intermediate focal plane of the separator. A schematic view of the experimental setup is given in fig. 1 (for more details see [24]).

The measured change of the magnetic rigidity of ions before and after they passed through a wedge-shaped degrader, placed at the intermediate focal plane of the FRS, was used to obtain unambiguous charge identification. In order to maximise the percentage of fully stripped ions, niobium stripper foils were placed after both the target and the wedge degrader.

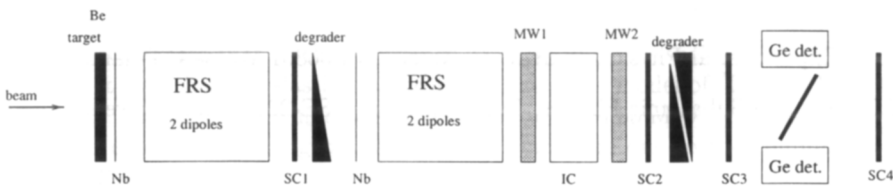


Figure 1. Schematic view of the experimental setup.

The mass-to-charge ratio of the ions,  $A/q$ , was determined from their time of flight through the second half of the FRS, as determined by scintillator (SC) detectors placed at the intermediate and final focal planes, and their x-position, measured with the same scintillators and additional multi-wire (MW) proportional counters. From a measurement of the energy loss of the fragments in an ionisation chamber (IC) placed at the final focus, the proton number,  $Z$ , could be obtained. The identified ions were subsequently slowed down in a variable thickness aluminium degrader followed by a scintillator detector, and finally stopped in a few mm thick catcher foil.

In order to distinguish and suppress events where the heavy ions were destroyed due to nuclear reactions in the degrader, the energy-loss signals in scintillator detectors placed upstream of the degrader and directly in front of the catcher were compared (see fig. 1.). Ions not stopped in the catcher were identified by a veto scintillator detector placed directly downstream of the implantation setup.

A gamma-ray detector array, consisting of segmented clover germanium detectors was positioned at the final focus of the FRS to detect gamma-rays in delayed coincidence with the implanted heavy ions. The delayed ion- $\gamma$ -ray coincidence range was 0–80  $\mu\text{s}$ . In order to minimise dead-time losses and avoid accidental ion-gamma coincidences, the total transmitted ion rate was kept below 1 kHz.

## 3. RESULTS

The first experiment using the described method to study isomeric decays in heavy ions was led by M. Pfützner [19]. Following the fragmentation of a  $1 \text{ GeV} \times A$   $^{238}\text{U}$  beam, the isomeric decays in  $^{212}\text{Pb}$  and neighbouring nuclei were observed. In 1999 a set of experiments were performed using a  $1 \text{ GeV} \times A$   $^{208}\text{Pb}$  beam in order to study both

neutron-rich nuclei (an identification plot is presented in fig. 2) and proton-rich nuclei [25]. The highlights of the experiment included the first observation of  $\gamma$ -ray transitions in the neutron-rich nuclei  $^{188}\text{Ta}$  [26,27],  $^{190}\text{W}$  [20],  $^{192}\text{Re}$  [26–28],  $^{198}\text{Ir}$  [26,28],  $^{201,202}\text{Pt}$  [26,27,29]. Further experiments using a  $^{238}\text{U}$  beam (at energies of  $750\text{ MeV}\times A$  and  $950\text{ MeV}\times A$ ) were performed in late 2001 and summer 2002, with the aim of studying neutron-rich nuclei with  $82 < Z < 92$ , and shape coexistence in the neutron-deficient lead region [30]. (In all these campaigns projectile-fission products around  $^{132}\text{Sn}$  were also studied [23].)

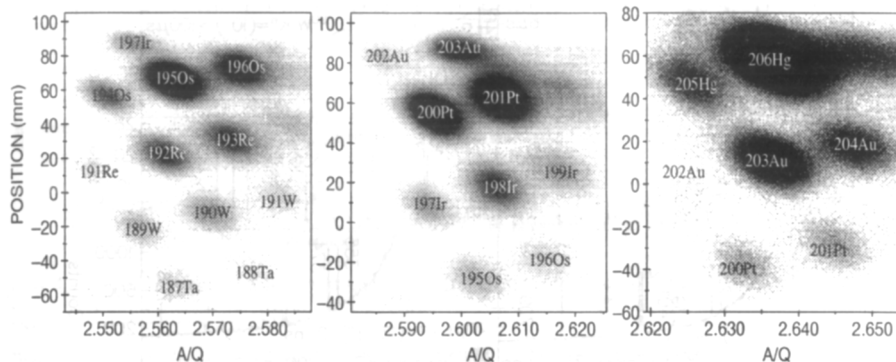


Figure 2. Identification plot (position at the final focus versus  $A/Q$ ) for the setting centred on  $^{191}\text{W}$ . The three figures show the fully stripped, H-like and He-like ions, respectively.

Representative  $\gamma$ -ray spectra, illustrating the power of the isomer decay method following projectile fragmentation, are presented in fig. 3. The wide range of isomers observed includes: the close to proton drip-line nucleus  $^{138}\text{Gd}$ , neutron-rich  $^{190}\text{W}$ ,  $^{200,201,202}\text{Pt}$  nuclei; isomers with half-lives between  $\approx 10$ – $20$  ns in  $^{200,201}\text{Pt}$  and larger than  $100\ \mu\text{s}$  in  $^{190}\text{W}$  and  $^{202}\text{Pt}$ ; spherical ( $^{194}\text{Pb}$ ) and oblate ( $^{188}\text{Hg}$ ) isomers in the neutron-deficient lead region. A  $\gamma$  gated coincidence spectrum of  $^{201}\text{Pt}$  is also shown.

The observation of isomeric decays provides an unique tool for the investigation of the angular momentum input of projectile fragmentation reactions. The population of isomeric states, ranging from the neutron-deficient  $^{138}\text{Gd}$  to the neutron-rich  $^{202}\text{Pt}$  following the fragmentation of  $^{208}\text{Pb}$ , was studied [24]. A similar investigation is under way for neutron-deficient isomers observed in the fragmentation of  $^{238}\text{U}$  [30].

#### 4. EXPERIMENTAL CONSIDERATIONS

The fragments arrive at the final focus of the FRS at relatively high energies, of the order of a few hundred  $\text{MeV}\times A$ , therefore the slowing down process gives rise to a high flux of bremsstrahlung radiation [31]. The detection of this prompt bremsstrahlung reduces the effective efficiency of the gamma-ray detection. Since with the use of conventional electronics no two gamma rays can be observed in a single Ge crystal in the same event, the affected detector cannot be used for the delayed gamma rays. This ‘blinding’ of the detectors is very severe, often reducing the efficiency by more than a factor of two. The distributions of the number of hit crystals (out of the total of 16) associated with the nuclei

of fig. 2 which survive the slowing down process are shown in the upper panels of fig. 4. These distributions are shown both as measured with ADCs (energy measurement with the condition that  $E_\gamma < 2$  MeV) and as measured with TACs (time measurement with no energy condition on the higher end). One can observe that the average multiplicity is higher for ions which are implanted at higher energies into the stopper. (The fully-stripped ions have lower  $Z$ , see fig. 2, therefore they are not slowed down so much in the degrader as the higher- $Z$  H-like and He-like ions).

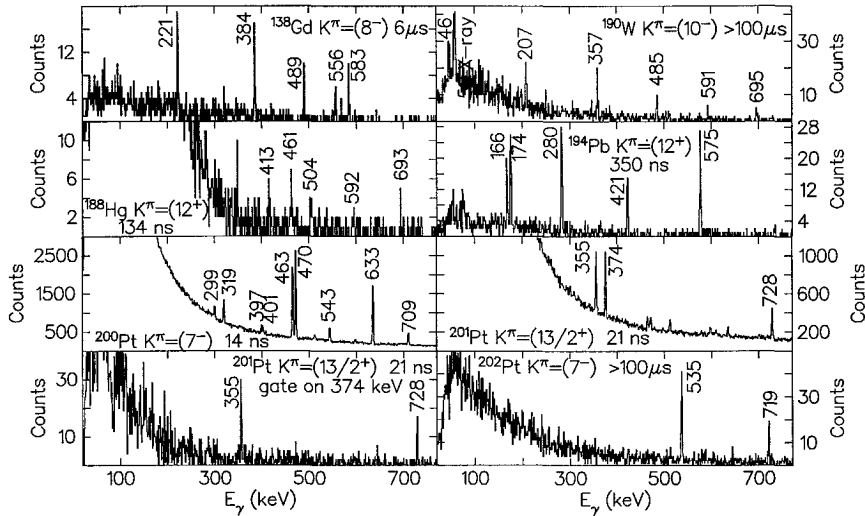


Figure 3. Examples of ion-gated  $\gamma$ -ray spectra (for details see the text).

A number of ions are destroyed during the slowing-down process in the degrader. The multiplicity distributions corresponding to these ions are presented in the lower panels of fig. 4. There is a striking difference between those measured with ADCs and TACs. This difference can possibly be understood as being caused by light particles hitting the Ge detectors. These light particles were created during the destruction of the heavy ions in the degrader, more than 1 metre from the Ge detectors. Since half of the crystals do not directly “see” the degrader, the high multiplicity in the TACs indicates that these particles penetrated through the whole thickness of the Ge detectors (233 MeV protons can pass through 10 cm of Ge). This interpretation is also supported by the study of the multiplicity measured with a BGO shield surrounding one of the Ge clovers. The flux of these light particles can be attenuated and in later experiments was drastically reduced by using lead-brick shielding.

The prompt background radiation has three components with atomic origin, namely: radiative electron capture (REC: when an electron of the target is captured in a bound state of the projectile), primary bremsstrahlung (PB: a target electron is captured in a continuum state of the projectile) and secondary bremsstrahlung (SB: from a collision between a target electron and the projectile). The properties of the components of the atomic background are listed in Table. I. In general there is a good agreement between the calculated and measured bremsstrahlung radiation [31]. However, there is a discrepancy:

in the case of the primary bremsstrahlung the magnitude of the measured cross sections is larger by a factor of  $\approx 2$  than the calculated value [31,32].

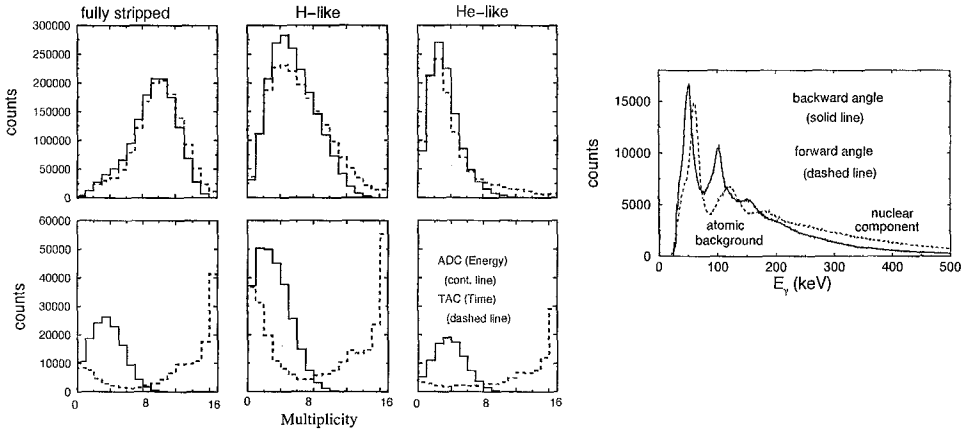


Figure 4. Distribution of Ge crystal hit multiplicity (for details see the text), and prompt background measured at  $\approx 60^\circ$  and  $\approx 120^\circ$ .

The measured prompt radiation is presented in fig. 4. We cannot easily compare with the calculations, since our background originates from many sources (but mainly the Al degrader and stopper). The asymmetry between the spectra at photon energies above a few hundred keV, taken at forward and backward angles, indicates its nuclear origin.

### 5. OUTLOOK

The RISING array consisting of 15 cluster detectors, presently part of EUROBALL, will start to operate at the final focus of the FRS in 2003. The high efficiency Ge-detector array together with the development of new particle tracking detectors have the objective to carry out, in addition to isomer decay measurements, new types of experiments, using fast ( $>100 \text{ MeV} \times \text{A}$ ) and slowed-down ( $4\text{-}20 \text{ MeV} \times \text{A}$ ) radioactive beams. Coulomb excitation of ground and isomeric states, nucleon removal and nucleon transfer studies, for example,

Table 1

Components of the atomic background and their properties [31].  $Z_p$  and  $Z_t$  are the atomic numbers of the projectile and target, respectively.  $E_b$  is the binding energy of the electron in the projectile (see the text for details).

Component	energy	Doppler shift	$\sigma(\theta)$	$\sigma(Z_p, Z_t, v)$
REC	$[(\frac{1}{\sqrt{1-\beta^2}} - 1)mc^2 + E_b] \frac{\sqrt{1-\beta^2}}{1-\beta\cos\theta}$	yes	$\sin^2\theta$	$Z_p^2 Z_t / v_p^5$
PB	$< (\frac{1}{\sqrt{1-\beta^2}} - 1)mc^2 \frac{\sqrt{1-\beta^2}}{1-\beta\cos\theta}$	yes	$\sin^2\theta(1 - \beta\cos\theta)$	$Z_p^2 Z_t / v_p^2$
SEB	$< 2 \frac{\beta^2}{1-\beta^2} mc^2$	no	isotropic	$Z_p^2 Z_t^2 / v_p^2$

will be performed for the first time for heavy nuclei produced in relativistic projectile fragmentation.

### Acknowledgements

The present paper presents results from several experiments. We would like to thank all those who were involved in these measurements.

### REFERENCES

1. I. Tanihata *et al.*, Phys. Rev. Lett. **55** (1985) 2676.
2. M. Lewitowicz *et al.*, Phys. Lett. **B332** (1994) 20.
3. R. Schneider *et al.*, Z. Phys. **A348** (1994) 241.
4. T. Motobayashi *et al.*, Phys. Lett. **B346** (1995) 9.
5. H. Scheit *et al.*, Phys. Rev. Lett. **77** (1996) 3967.
6. R. Grzywacz *et al.*, Phys. Lett. **B355** (1995) 439.
7. M. Bellegric *et al.*, Nucl. Phys. A **682** (2001) 136c.
8. D. Sohler *et al.*, Phys. Rev. **C66** (2002) 054302.
9. H. Okuno *et al.*, Phys. Lett. **B354** (1995) 41.
10. G. Neyens *et al.*, Nucl. Phys. **A682** (2001) 241c.
11. K. Yoneda *et al.*, Phys. Lett. **B499** (2001) 233.
12. M. Stanoiu *et al.*, to be published.
13. J. Giovinazzo *et al.*, Phys. Rev. Lett. **89** (2002) 102501.
14. H. Geissel *et al.*, Nucl. Inst. Meth. B **70** (1992) 286.
15. M. Zinser *et al.*, Phys. Rev. Lett. **75** (1995) 1719.
16. M. Schäfer *et al.* Phys. Rev. **C57** (1998) 2205.
17. S. Wan *et al.*, Z. Phys. **A358** (1997) 213.
18. W.-D. Schmidt *et al.*, Z. Phys. **A350** (1994) 215.
19. M. Pfützner *et al.*, Phys. Lett. B **444** (1998) 32.
20. Zs. Podolyák *et al.*, Phys. Lett. B **491** (2000) 225.
21. M. Pfützner *et al.*, Eur. Phys. J. A **14** (2002) 279.
22. M. Bernas *et al.*, Phys. Lett. **B415** (1997) 111.
23. M.N. Mineva *et al.*, Eur. Phys. J. **A 11** (2001) 9.
24. M. Pfützner *et al.*, Phys. Rev. **C65** (2002) 064604.
25. Zs. Podolyák *et al.*, in: C.M. Petrache, G. Lo Bianco (Eds.), Proc. of the conf. ‘Exotic Nuclei at the Proton-Drip Line’, University of Camerino, 2001, p.189.
26. Zs. Podolyák *et al.*, in: J.H. Hamilton, W.R. Phillips, H.K. Carter (Eds.), Proc. of the Int. Conf. on Fission and Properties of Neutron-Rich Nuclei, World Scientific, p. 156.
27. M. Caamaño *et al.*, Nucl. Phys. **A 682** (2001) 223c.
28. P. Mayet *et al.*, in: AIP Conf.Proc. **610** (2002) p. 761.
29. Zs. Podolyák *et al.*, Progress of Theoretical Physics (in press).
30. K. Gladnishki *et al.*, Acta Physica Polonica A (in press).
31. R. Anholt *et al.*, Phys. Rev. **A33** (1986) 2270.
32. H. Tawara *et al.*, Phys. Rev. **A55** (1997) 808.